UNIVERSITY OF BIRMINGHAM

6th Annual

BEAR

Postgraduate Researcher Conference 2015

Numerical Modelling and Its Applications in Natural Sciences and Engineering

Contents

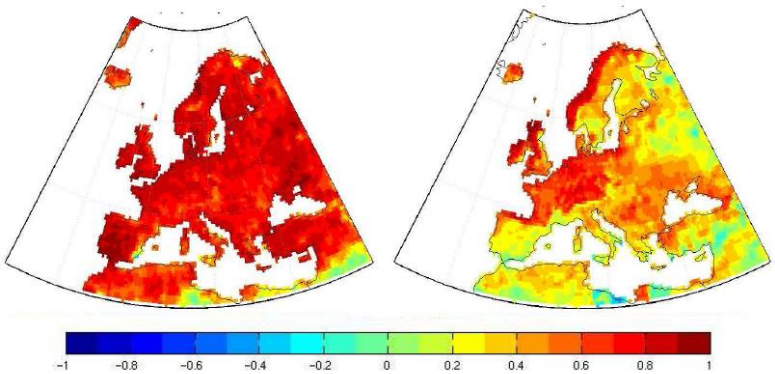

Developing a correction for simulated rainfall from global climate change models – Jonathan Eden, School of Geography, Earth ad Environmental Sciences

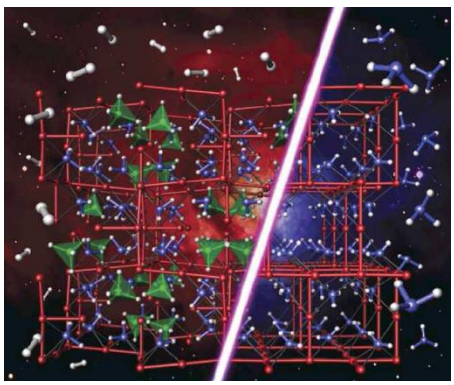

Biocatalysis for applications in PEM fuel cells - Paul Jennings, School of Chemical Engineering

Welcome

Welcome to the University of Birmingham and to the sixth annual BEAR PGR conference. The conference is organised by postgraduate researchers from across the University. There are a diverse range of research themes across the University and the BEAR conference offers an opportunity for researchers from all disciplines to come together and share their experiences of research undertaken using numerical modelling.

The University of Birmingham encourages and facilitates multidisciplinary research, education and development over a wide range of fields. In order to reach that goal, effective dissemination of high quality research is necessary. This is done through the hosting of regular conferences and workshops which assist in the transfer of knowledge and good practice to the academic and industrial communities. The purpose of this conference is to promote the exchange of the latest information and developments in various fields, all underpinned by a common interest in numerical modelling and its applications in natural Science and Engineering.

This is the sixth conference in the series of annual events that provide an excellent opportunity for scientists, engineers and other academic researchers to come together as one community. The event builds on the success of the previous conferences held annually in Birmingham since 2010. Thanks to an excellent response to the call for papers, the Organising Committee has put together a wide ranging programme. We are delighted that so many researchers are keen to share their work with their. We look forward to a stimulating event that is beneficial to all.

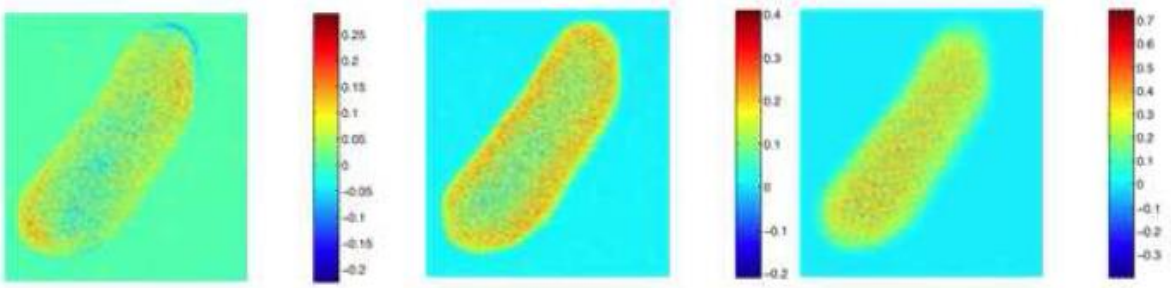

Cross-Correlation Nanoparticle Tracking for 2D Spatial Drift Correction in Post-acquisition Analysis – Dongsheng He, School of Physics and Astronomy

Agenda

09:30-10:00	Registration
10:00-10:20	**Welcome talk** **Jean-Baptiste** *Centre for Computational Biology, University of Birmingham*
10:20-11:00	***Plenary talk*** **Ben Brown** *Laurence Berkeley National Labroratory, California*
11:00-11:15	**Fadhel Al-Mousawi** "*Performance Evaluation of Multi-bed Silica gel Adsorption System for Cooling and Power Generation*"
11:15-11:30	**Jim Barrett** "*CARMA models for stochastic variability*"
11:30-12:00	*Coffee*
12:00-12:40	***Plenary talk*** **David Smith** *School of Mathematics, University of Birmingham*
12:40-12:55	**Kristian Brock** "*A Design for Phase II Clinical Trials with Efficacy and Toxicity Outcomes and Predictive Variables*"
12:55-13:40	*Lunch*
13:40-14:00	**Poster session**

14:00-14:10	*Photo*
14:10-15:00	***Plenary talk*** **Ben Saunders and Nils Warnken** *Rolls-Royce plc and University of Birmingham*
15:00-15:15	**Muhammad Subkhi Sadullah** "*Ternary Lattice Boltzmann simulation for Modelling Lubricant Impregnated Surfaces* "
15:15-15:30	**Stefanie Gillmeier** "*An overview of our currently used tornado-like vortex models*"
15:30-15:50	*Coffee*
15:50-16:05	**Andrew Edmondson** "*Discovering new family trees of biblical manuscripts Department of Theology and Religion*"
16:05-16:20	**Austin Tomlinson** "*Accelerating the Vortex Lattice with CUDA*"
16:20-17:00	***Plenary talk*** **John Easton** *Chief technology officer, IBM Systems and Technology Group*
17:00-17:30	**Prizes and Closing remarks**

Plenary speakers

Jean-Baptiste Cazier

Centre for Computational Biology, University of Birmingham

Jean-Baptiste Cazier is a Professor of Bioinformatics with interest across the broad spectrum of Computational and Mathematical modelling of natural phenomena. He has three main area of interest: Cancer Genetics, Population Genetics, Swarming and Metabonomics. His life-long goal is to integrate all his eclectic, and ever expending, fields of interest.

James "Ben" Brown

Laurence Berkeley National Labroratory, California

Ben Brown is a statistical biologist with diverse interests ranging from ecotoxicology to developmental biology. A common theme uniting his work is the study of gene regulation. His lab develops statistical machine learning tools to elucidate regulation in basal and ecologically adverse conditions.

Ben joined the Life Sciences Division in 2013 where he and his team are building a program focused on the development of tools for the integrative analysis of large, multi-scale biological datasets.

In 2015, he joined the UCB Statistics faculty as an adjunct professor to further his work on ensemble models. In the modENCODE Consortium, he led analysis for the fly transcription consortium (2011-2014).

David Smith

School of Mathematics, University of Birmingham

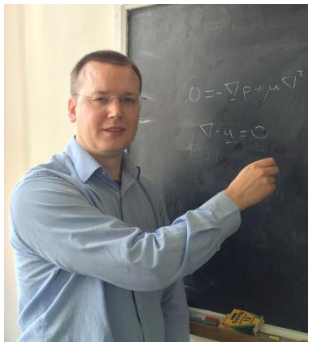

David J. Smith is Senior Lecturer in Applied Mathematics and Head of the Applied Mathematics research group.

Dave's main research areas are sperm motility biofluiddynamics, working alongside Centre for Human Reproductive Science, Birmingham Women's Hospital, and modelling the synthetic biology nanofiber M13 bacteriophage. Another central area of interest is the related problem of how cilia shape the development of the growing embryo.

Dave is an enthusiastic communicator of applied mathematics and biological modelling, and provides talks to young people on this subject, including recent school and college visits, and organises IMA West Midlands Branch talks at the University of Birmingham.

Ben Saunders

Team Leader - Materials & Process Modelling, Rolls-Royce plc

Ben Saunders graduated from University of Leeds with a Master degree in Automotive Engineering in 2004. Following a short stint at Ford Motor Company he joined Rolls-Royce plc in 2005 as a Finite Element Analysis Engineer, developing & validating heat transfer models for use in engine certification & component design. In 2011 Ben took on the role of managing the Materials & Process Modelling team within Design Systems Engineering, focussing on the development & validation of new & novel Material & Manufacturing Process simulation tools and deploying these capabilities across Rolls-Royce.

Nils Warnken

School of Metallurgy and Materials, University of Birmingham

Nils Warnken graduated from RWTH-Aachen University, Germany, in 2007 with a Dr.Ing. In Metallurgy and Materials Engineering. He is now a lecturer at the School of Metallurgy and Materials at the University of Birmingham. His research interest is the study and modelling of phase-transformation in metals and alloys, with a special interest in solidification related phenomena.

John Easton

Chief technology officer, IBM Systems and Technology Group

John Easton is an IBM Distinguished Engineer and the chief technology officer for IBM Systems and Technology Group in the UK and Ireland. He is known for his work helping commercial clients exploit large-scale distributed computational infrastructures. John currently leads a European team of IBM architects building the next generation of systems infrastructures to support business analytics workloads.

Student presentations

Fadhel Al-Mousawi

Performance Evaluation of Multi-bed Silica gel Adsorption System for Cooling and Power Generation (Fadhel Al-Mousawi, Raya Al-Dadah, Saad Mahmoud)

Global power demand has increased significantly over the last few decades and the need for sustainable sources has become an urgent aim. Low grade heat sources such as solar energy, geothermal energy and waste heat can be alternative sources. Silica gel/water adsorption for cooling and power could be a promising low-grade heat utilization system because of its ability to use low grade heat below 358 K. In this study, the basic adsorption cooling cycle has been modified by adding an expander between the hot bed and the condenser to generate electricity as well as cooling. A MATLAB Simulink program for multi bed Silica gel water adsorption system for cooling and power has been developed to investigate the effect of using different number of beds on the overall cycle performance. Results show that it is possible to produce power and cooling at the same time without affecting the cooling output. Results show that for 3 and 4 bed adsorption system can produce average cooling and power of almost 2.65 kW and 0.27 kW and 3.43 kW and 0.36 kW respectively compare to 1.63 kW cooling and 0.17 kW using 2 bed adsorption system. In addition, the COP and the total cycle efficiency have been investigated at different operating conditions.

Jim Barrett

CARMA models for stochastic variability

Stochastic variability is one of the most important concepts in experimental physics. There are almost no experiments where measurement errors don't matter, and there are many interesting physical systems that are so complicated that our observations of them can look like a stochastic mess. In my talk I present a method for making sense of stochastic variability using continuous, autoregressive moving average (CARMA) models, which allow us to efficiently pin down the intrinsic timescales in a stochastic process. I'll also show how I've used CARMA models, Bayesian inference and a whole bunch of computing power to investigate planets around distant stars, stellar winds and the orbit of a neutron star.

Kristian Brock

A Design for Phase II Clinical Trials with Efficacy and Toxicity Outcomes and Predictive Variables

PePs2 is a phase II clinical trial of Pembrolizumab in non-small cell lung cancer patients. The primary objective is to learn if treatment is associated with sufficient efficacy and acceptably-low toxicity to be given to performance status 2 patients. Patient-specific factors will likely affect whether patients achieve a good outcome. Two predictive variables of note are the expression level of the PD-L1 protein; and whether the patient has been treated before.

Existing phase II trial methodologies simultaneously scrutinise efficacy and toxicity but do not admit predictive variables. Can we create a design that uses predictive data to selectively approve the treatment only where it works?

We developed a novel Bayesian methodology called BeBoP that analyses binary efficacy and toxicity outcomes. Importantly, BeBoP admits explanatory variables so we could control for the fact that patients have different PD-L1 expression levels. Using a broad simulation study, we demonstrated that BeBoP performs well across a wide range of scenarios. BeBoP let us avoid the unappealing prospect of running separate trials for good and poor prognosis patients.

Bayesian statistics fuses prior beliefs with observed data and involves calculus. The update integral in our example is five-dimensional and costly to evaluate. Each iteration evaluated eight such integrals. We studied 16 scenarios and performed 10,000 replicates, so 1.28m integrals were evaluated. If each took 1s, this would require 15 days of processing. We completed the simulations in less than a day thanks to the massive opportunity for parallel processing in BEAR.

Muhammad Subkhi Sadullah

Ternary Lattice Boltzmann simulation for Modelling Lubricant Impregnated Surfaces

Lubricant Impregnated Surfaces (LIS) are porous surfaces infused with lubricant (e.g. oil). Compared to superhydrophobic surfaces, LIS have been demonstrated to have superior range of liquid repellency as well as better robustness. Given such advantages, LIS have many promising applications varying from foods and beverages packaging to energy harvesting systems. Investigating such system empirically is demanding as it is subject to surface texturing, surface energy manipulation, and the availability of the lubricant. To complement experiments, a powerful numerical approach is therefore needed. In this contribution we present a ternary free energy lattice-Boltzmann model suitable for simulating such system. The distinctive feature of this free energy model is that we are able to predict analytically and capture the relevant physical parameters such as contact angles, liquid-liquid and solid-liquid interfacial tensions. To verify the consistency of this free energy model, we first performed wetting simulation of two immiscible liquids on a solid surface and confirmed its agreement with the so called Girifalco-Good relations. The model is then exploited to map possible wetting states in LIS system as predicted by simple thermodynamic argument. We then discuss how the wetting behaviour of water droplets on LIS may depend on the initial condition and their wetting states.

Stefanie Gillmeier

An overview of our currently used tornado-like vortex models (Stefanie Gillmeier, Hassan Hemida and Mark Sterling)

The structure of a full-scale tornado is highly complex, showing a three-dimensional flow field, instabilities, singularities and non-linear effects. Whether a vortex model can represent the complexity of a real tornado depends on the similarity of the model solution to the full-scale case. However, data sets of full-scale tornadic events are very limited and for that reason tornado-like vortices are modelled numerically and experimentally to provide a statistical representative validation data set for different vortex models. At the School of Civil Engineering ANSYS CFX commercial code is used as a simulation tool to study tornado-like vortices. The design consists of two chambers, a convection chamber and a convergence chamber. Angular momentum is imposed by guide vanes around the convergence chamber. Different vortex structures can be produced by changing the guide vane angle. Experimental simulation in a similar shaped tornado-like vortex simulator are conducted and used to validate the numerical model. Current interest of research is to use those numerical and experimental simulations to analyze the effect of scaling on wind loads on structures exposed to tornado-like flow fields. This conference contribution provides an overview about what can and will be done regarding tornado research at the University of Birmingham throughout the next years.

Andrew Endmondson

Discovering new family trees of biblical manuscripts Department of Theology and Religion

Until the arrival of the printing press, all documents had to be copied by hand – and the copyists made mistakes every time. These changes in the text are analogous to genetic mutations in species' DNA. Therefore the tools used in the field of phylogenetics to study the evolution of species can also be used to study the evolution of texts of a given work. The International Greek New Testament Project transcribed 1,659 manuscripts of chapter 18 of the Gospel of John into electronic form, which were then collated using specialist software. I encoded this data into a matrix (with over 650,000 pieces of information) suitable for input to the phylogenetic software "MrBayes". MrBayes is a powerful open source application that runs the Metropolis-Coupled Markov Chain Monte Carlo (MC3) algorithm to perform Bayesian inference for phylogenetic and evolutionary models. It is MPI-capable, and therefore highly suitable for making use of BlueBEAR's parallel processing. The resulting phylogenetic tree for John 18 contains many interesting features. For example, one sub-tree corresponds to the famous "Ferrar Group" of New Testament manuscripts. Here the group membership identified by MrBayes agrees with the conclusions of recent more traditional research – even though all the known criteria for group membership are found elsewhere.

Austin Tomlinson

Accelerating the Vortex Lattice with CUDA.

When simulating the melting of a superconducting vortex lattice, computational optimisations are crucial for achieving reasonable run times. The vortex lattice consists of two-dimensional magnetic flux tubes in a regular array. We are interested in how these lattices “melt” into “vortex liquids”. This field is particularly prone numerical artefacts that are consequences of the system having very long transient behaviour and sensitivity to the size of the system. Typically, we gain excellent speed-ups of the required code by parallelizing our molecular dynamics engine. By modifying our serial code using Intel® Cilk™ Plus, we achieve optimal performance on BlueBEAR’s standard nodes. When scaling up our problem to larger numbers of vortices, we search for new ways to accelerate our code. CUDA is a C/C++ extension developed by NVidia to enable developers to program their graphics cards. The GPUs on BlueBEAR’s GPU service offer Tesla K20 cards with over 2000 cores that we can simulate the vortex lattice on. We are one of few adopters of this service and are innovating new ways to simulate vortex physics. GPU acceleration is more involved than CPU parallelization; there is a hierarchy of slow global memory to a fast local cache. Memory management is key to achieving optimal run times, as is careful control of thread distribution. We will discuss how we have implemented CUDA in the context of the vortex lattice, quantify the efficiency of GPU acceleration for this problem, and how it relates to the BlueBEAR setup.

Student posters

 # 1 Manal AlQhtani

The Numerical Integration Problem in Ecological Monitoring

 # 2 Yousif Al-Sagheer

Nonlinear Model Predictive Control (NMPC) for PEM Electrolyser

 # 3 Mostapha Ariane

Smoothed Particle Hydrodynamics Based Modelling for Blood Flow in Heart and Vein Valves

 # 4 Kamal Nayan Goswami

Ab Initio Study of the Effect of Solute Atoms on the Vacancy Diffucion in Ni-Based Superalloys

 # 5 John Hey

Geometry and Conferred Ordering Within Hydrated Perchlorate Clusters

 # 6 Carolina Eleonora Lavecchia

Parametric Finite Element Model of the Human Lumbar Spine

 # 7 Zainab Shukur

The Friction Coefficient and Wears Mechanisms of PEEK and PEEK Composite in Water Lubricated Sliding Contacts

 # 8 Jiejie Wu

Finite Element Modelling of CRUD Deposition in Nuclear Plant Utilising COMSOL Multiphysics

 # 9 Wenxin Zuo

Application of a Ghost Fluid Approach for a Multiphase Lattice Boltzmann method

The Numerical Integration Problem in Ecological Monitoring

M. M. Alqhtani and N. B. Petrovskaya
MMA249@student.bham.ac.uk , N.B.Petrovskaya@bham.ac.uk
School of Mathematics, University of Birmingham, Birmingham, B15 2TT, UK

Introduction

- The numerical integration methods are used to evaluate the following integral: $I = \iint_D f(x,y)dxdy$;

  when the exact value of integral is not available.
- In many practical problems numerical integration methods are applied to experimental data. One of such problems is the problem of pest monitoring and control. In the latter case the integrand $f(x,y)$ is the pest population density and the integral gives the total number of pests in the domain (pest abundance).
- As a result of obtaining data from experimental measurements the function values required for integration are only available at several locations over the domain.
- In ecological applications an accurate estimation of pest abundance is vital to determine if control action is required, see [5].
- The density $f(x,y)$ is measured by a trapping procedure where traps are placed at nodes of a regular grid. The number of traps is usually small because of financial and labor restrictions.
- In ecological situation, the grid cannot be refined to gain more accurate estimation of pest population density because the same measurement conditions cannot be recreated.

Method

- The population density $f(x) \equiv f(x_i)$ is available at grid nodes (x_i); $i = 0, \dots, N$.
- The following integral has to be computed:
  $$I = \int_a^b f(x)dx.$$
- The regular computational grid nodes is generated as:

  $x_{i+1} = x_i + h_i$; where $x_1 = a$, $x_N = b$, $h_i > 0$ is the grid step size.
- The Lagrange interpolating polynomial is used to approximate the function f(x) as :
  $$p_n^j(x) = \sum_{j=0}^{n} f_j \left| \prod_{k=0}^{n} \frac{x - x_k}{x_j - x_k} \right|$$
- Then the integral is approximated at each sub-interval by using Lagrange interpolating polynomial of degree n:
  $$I_i = \int_{x_{i-1}}^{x_i} f(x)dx \approx \int_{x_{i-1}}^{x_i} p_n^i(x)dx = I_i.$$

Future Work

- Investigate the effect of grid randomness on the degree of accuracy for standard and ecological test cases.
- Seek to provide more accurate methods to deal with sparse ecological data.

Objectives

- The pest abundance has to be evaluated by integrating the density function obtained via the trapping mechanism.
- The threshold number of traps required for an accurate estimation of pest abundance has to be found.
- The problem in one dimension will be considered firstly, then the methodology will be extended to the two-dimensional cases.
- The numerical integration methods will be modified to evaluate the pest abundance for heterogeneous spatial density distributions.

Method Validation

- The integration error on a regular grid can be defined as:
  $$|E_n(x)| \leq C_n h^{n+1} \quad (e.g. see [3]).$$
- By plotting the relative error E against the number of subintervals $N-1$ we obtained convergence graphs for various numerical integration methods.
- Convergence curves of the trapezoidal rule, Simpson's rule, Richardson extrapolation for trapezoidal rule and Richardson extrapolation for Simpson's rule are plotted for comparison .
- On all standard mathematical test cases the convergence of Simpson's rule is the fastest; see Figure 1.
- For an integrand function with a simple spatial pattern the convergence rate can already be seen on coarse meshes.
- For more complicated cases the convergence rate estimate does not hold on coarse grids. A grid has to be refined to achieve convergence estimates.
- The Richardson extrapolation works effectively for standard mathematical test cases; see Figure 1.

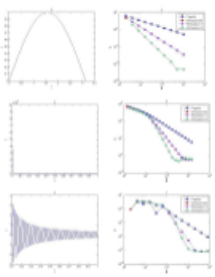

Figure 1: standard mathematical test cases.

Ecological results

- Ecological data are generated from the (dimensionless) Rosenzweig-MacArthur model ; see [2]:

  $$\frac{\partial u(x,t)}{\partial t} = d\frac{\partial^2 u}{\partial x^2} + u(1-u) - \frac{uv}{u+h};$$

  $$\frac{\partial v(x,t)}{\partial t} = d\frac{\partial^2 v}{\partial x^2} + k\frac{uv}{u+h} - mv.$$
- The 'exact' solution I_N is be computed on the finest available grid where the number of nodes is $N_f = 2^{15}+1$.
- The numerical integration methods are applied on each coarse grid extracted from finest grid.
- The integration error has the following form:
  $$E = \frac{|I_{Nf} - I_{Nc}|}{I_{Nf}}.$$

Where I_{Nf} is the exact value of integral and I_{Nc} is the approximate value obtained on a coarse grid.

- It can be seen from figure that the numerical integration methods do not present satisfactory degree of accuracy.
- The Richardson extrapolation has been applied to improve the accuracy. However, it demonstrated poor performance; see Figure 2.

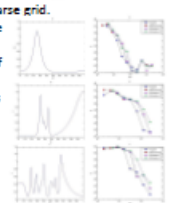

Figure 2: Convergence curves of the numerical integration methods and the Richardson extrapolation for various ecological test cases on a regular grid.

Conclusions

- In the mathematical test cases the numerical integration methods can be more accurate than statistical methods.
- The Richardson extrapolation may have a higher degree of accuracy in the (1-d) mathematical test cases
- An alternative approach must be applied to present an accurate estimation for the ecological problems when the data available is sparse.

References

1. P., Davis. Interpolation and Approximation. Blaisdell Publishing Company, New York, 1963.
2. J., Murray. Mathematical Biology: an Introduction, Volume 1. Springer,2002.
3. A., Quarteroni, et al. Numerical Mathematics. Springer Verlag, 2007.
4. J., Stoer, and R., Bulirsch. Introduction to Numerical Analysis. Springer-Verlag, New York, 1980
5. V., Stern. Economic thresholds. Ann Rev Entomol 18:259-280, 1973.

Nonlinear Model Predictive Control (NMPC) for PEM Electrolyser

Yousif Al-sagheer, Robert Steinberger-Wilckens
Centre for Fuel Cell and Hydrogen Research, School of Chemical Engineering
The University of Birmingham, B15 2TT, UK, *Email: YIW213@bham.ac.uk*

Introduction

A model for polymer electrolyte membrane (PEM) electrolyser (EL) and its controller is needed as part of an extended model of a plant of renewable energy sources (RES) integrated with hydrogen technology in order to study the feasibility of balancing RES fluctuations. The aim of the controller is to adjust electrolyser current so that the consumed energy by the electrolyser is consistent with surplus energy events. As the relation between the EL power and current is highly nonlinear, the need to nonlinear controllers arises. A model predictive control (MPC) algorithm is applied for PEM EL operation in simulation environment, depending on predictions from the EL nonlinear model.

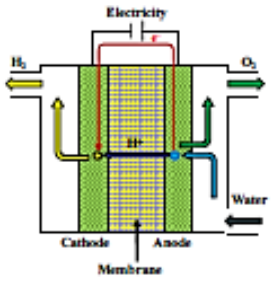

PEM Electrolyser

$H_2O + \text{electricity} \rightarrow 2H_2 + O_2$

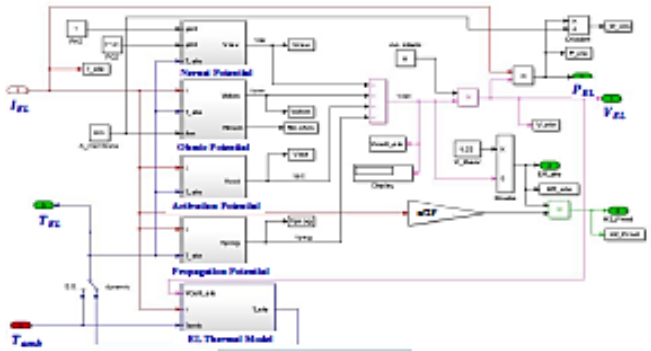

Simulink EL models

Cost Function & Constraints

$$J = W_p \sum_{i=1}^{n_y} \left\| Pst_{k+i} - P_{EL,k+i} \right\|_2^2 + W_{\Delta I} \sum_{i=1}^{n_u} \left\| \Delta I_{EL,k+i} \right\|_2^2$$

All terms in "J" should be expressed in terms of the manipulated variables I_{EL} assuming $\Delta I_{EL} = 0$ after control horizon n_u

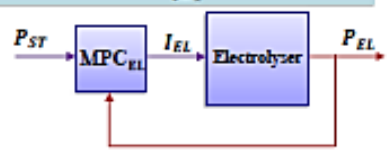

$$\min_{I_{EL}} J(I_{EL}) \text{ subject to } \begin{cases} 0 \le I_{EL} \le I_{EL,max} & \text{Physical constraints} \\ I_{EL} = 0 \ (\text{if } P_{ST} < P_{EL,min}) & \text{Operator constraints} \\ \text{Any other constraint can be added} \end{cases}$$

Constraints need to be expressed in terms of I_{EL}

$$\min_{I_{EL}} J(I_{EL}) \text{ subject to } \begin{cases} -I_{EL,k+i} \le 0 \\ I_{k+i} \le I_{max} \\ I_{k+i} \times (P_{ST,k+1} < P_{EL,min}) = 0 \end{cases}$$

The Matlab Symbolic Math & Optimization toolboxes are used

Results

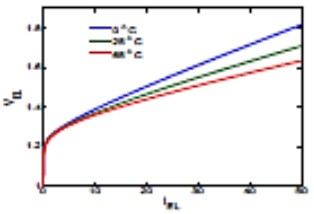

PEM EL polarization curves

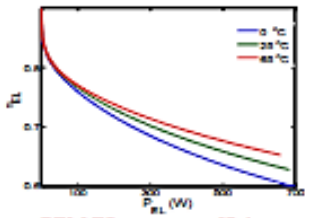

PEM EL power vs efficiency

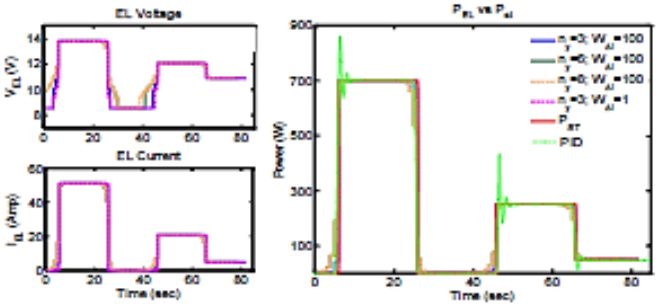

EL Response for different MPC parameters & PID controller

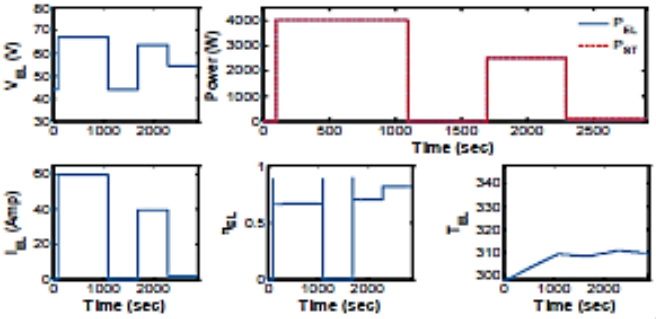

MPC response to different power set points with time

NMPC Algorithm

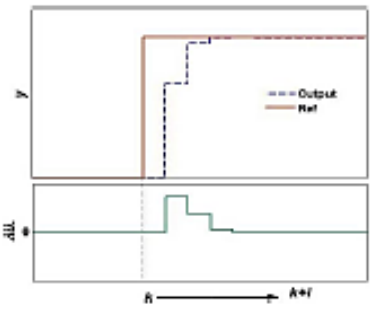

MPC Algorithm

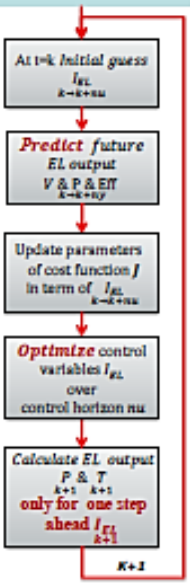

$$J = \sum_{i=1}^{n_y} \left\| r_{k+i} - y_{k+i} \right\|_2^2 + \sum_{i=1}^{n_u} \left\| \Delta u_{k+i} \right\|_2^2$$

$$\Delta u(k) = \min_{\Delta u = [\Delta u_0 \ldots \Delta u_{N-1}]} J \quad \text{subject to: Plant Constraints}$$

References

- Lebbal, M.E. and Lecoeuche, S. (2009) Identification and monitoring of a PEM electrolyser based on dynamical modelling. International Journal of Hydrogen Energy
- Gorgun, H. (2006) Dynamic modelling of a proton exchange membrane (PEM) electrolyzer. International Journal of Hydrogen Energy
- Golbert, J. and Lewin, D.R. (2007) Model-based control of fuel cells: (2): Optimal efficiency. Journal of Power Sources, 173 (1): 298–309
- Barbir, F. (2005) PEM Fuel Cells: Theory and Practice. Elsevier Academic Press
- Rossiter, J.A. (2003) Model- Based Predictive Control: A Practical Approach. CRC Press

Conclusions

- The MPC controller shows very good tracking for changes in power set-point.
- Very short rise time, even it can respond in advance, better rise time requires smaller sampling time and hence a powerful CPU.
- The MPC controller can handle and apply multiple performance indices.
- Formulating the cost function & constraints can reflect the operator objectives.
- The MPC controller keeps the EL in a safe operating region and does not violate operational constraints, in comparison to conventional PID controller.
- The MPC controller rejects system noise due to model imperfection by updating EL model regarding the temperature changes.

EPSRC Pioneering research and skills
UNIVERSITY OF BIRMINGHAM
Energy

Smoothed Particle Hydrodynamics based modelling for blood flow in heart and vein valves

Mostapha ARIANE and Alessio ALEXIADIS

School of Chemical Engineering College of Engineering & Physical Sciences University of Birmingham
Birmingham B152TT West Midlands United Kingdom

mxa437@bham.ac.uk

Purpose of the study

The blood system is both simple and complex. It is simple in that it can be compared to a flow in a tube permitting blood circulation in the whole of the human body, and it is complex due to several mechanisms involved (pulsatile flow, valve movements, etc). Hence, comprehension of these governing mechanisms by modelling is necessary in order to provide quick and complete responses.

State of art

Majority of blood flow modelling is conducted by mesh-based methods, either by Computational Fluid Dynamics (CFD) or more generally by Fluid Structure Interaction (FSI). However, it becomes limited when the flow is unstable such as under high velocity, and in particular during strong flow perturbation. Moreover, mesh-based methods require a re-mesh after each iteration which generates a significant increase in calculation time and cost.

Objectives

- Use of a Lagrangian than an Eulerian approach
  Smoothed Particle Hydrodynamics (SPH)
  - Particular technique
  - Mesh-free initialization
  - Local properties
- Simulation of valve movements amid blood flow in organic tissues
  - ⇒ Cardiac arteries
  - ⇒ Legs veins

Fundamentals

Representation of the function

Kernel approximation by summation [1]

$$f(r_i) = \sum_j m_j \frac{f_j}{\rho_j} W(r_i - r_j)$$

Where interpolating kernel W is a Gaussian and the smoothing length h is comparable to a few typical inter-particle spacing

$$P(\rho) = P_0 + \frac{c_0^2 \rho_0}{\gamma}\left[\left(\frac{\rho}{\rho_0}\right)^{\gamma} - 1\right]$$

Example of pressure calculation with Tait Equation of State (EOS) for free surface water flow modelling [2]

Integral interpolant of the field function $f(r_i)$

Particle approximation using particles within the support domain of the smoothing function W per (blue) [3]

Equations of conservation

Approximation of density

Summation density $\rho_i = \sum_j m_j \frac{\rho_j}{\rho_j} W_{ij} \equiv \sum_j m_j W_{ij}$ Continuity density $\frac{d\rho_i}{dt} = \sum_{j=1}^{n} m_j \rho_i \frac{\partial W_{ij}}{\partial x_i^{\beta}}$

Approximation of momentum

$$f_i = m_i \frac{dv_i}{dt} = -\sum_j m_j m_j \left(\frac{p_i}{\rho_i^2} + \frac{p_j}{\rho_j^2}\right) \nabla_i W_{ij}$$

Approximation of energy

$$m_i \frac{dv_i}{dt} = -\frac{1}{2}\sum_j m_j m_j \left(\frac{p_i}{\rho_i^2} + \frac{p_j}{\rho_j^2}\right) \cdot v_{ij} \nabla_i W_{ij} - \sum_j \frac{m_j m_j (\lambda_i + \lambda_j)(T_i - T_j)}{\eta_j} e_{ij} \cdot \nabla_i W_{ij}$$

Viscosity treatment

Artificial viscosity

Parameter added to the motion and energy equations [1]

$$\Pi_{ij} = -\alpha \bar{c}_{ij} \frac{\eta_i + \eta_j}{\rho_i + \rho_j} \frac{v_{ij} \cdot r_{ij}}{r_{ij}^2 + \varepsilon h^2}$$ ⇒ Stability of calculation

Sound speed approximation $\beta = \frac{\Delta P}{\Delta \rho_0} = \frac{|\rho - \rho_0|}{\rho_0} = \frac{V_0^2}{c^2} = M^2$ $\alpha = \frac{\eta_0}{\rho_0 c}$

Laminar flow viscosity [4]

Modification of the viscous term for increasing accuracy at low velocity

$$\left(\frac{1}{\rho}\alpha\beta\nabla\right)_i = \sum_j \frac{m_j(\alpha_i + \alpha_j)v_{ij} \cdot \nabla_i W_{ij}}{\rho_{ij}(r_{ij}^2 + \varepsilon h^2)} v_{ij}$$

Benchmark with water flow

Standard Poiseuille flow case

- Two parallel plates are stationary (orange particles)
- Water flow through walls (blue particles)
- 20 particles on the length X (5×10^{-4} m)
- 40 particles on the height Y (1×10^{-4} m)
- Constant driven body force of 2×10^{-4} m/s² in X direction
- Peak fluid velocity of 2.5×10^{-3} m/s

⇒ Reynolds number of 2.5×10^{-2}, *Laminar flow*

Initial geometry and particles distribution

series solution for the transient behaviour [4]

$$v_x(x,t) = \frac{\rho g}{2\mu}x(x-l) + \sum_{n=0}^{\infty} \frac{4\rho g l^2}{\mu\pi^3(2n+1)^3} \sin\left(\frac{n\pi}{l}(2n+1)\right) \exp\left(-\frac{(2n+1)^2\pi^2\mu}{\rho l^2}t\right)$$

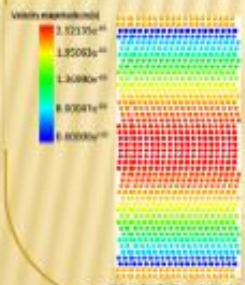

particles distribution at steady state

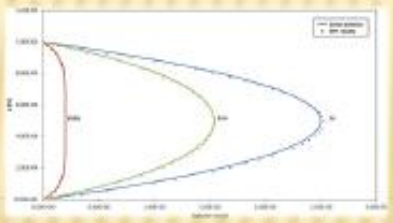

Velocity profiles at centre of flow for 0.01s, 0.1s and 1s (steady state)

Advantages

- Grid-free allowing a Local discretisation
- Each particle linked with neighbourhood
- Ease of carrying out of complex geometry
- Tracking of particles motion

Applications with blood flow

Leg venous valves

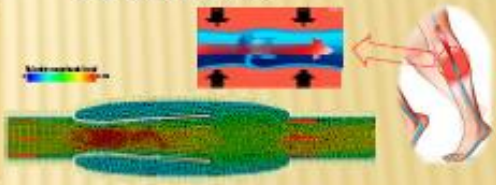

Heart valve movement during oscillating flow

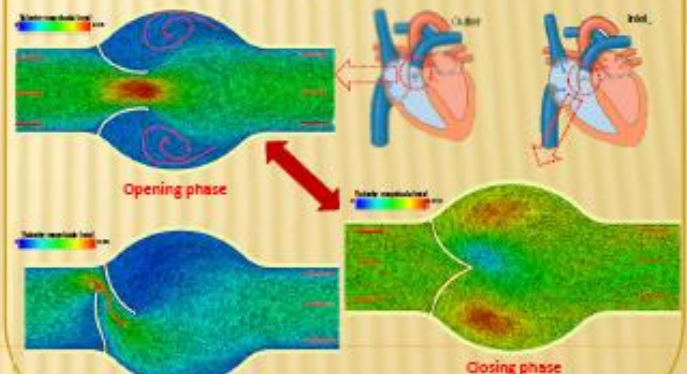

Dysfunction of valves due to prolapse disease

Perspectives

With the help of the SPH method (created initially for astro-physics problems [5][6]), different biological arteries and veins have been designed in 2 dimensions, in particular, by realistically simulating valve movements and their elasticity during an oscillating flow. The absence of mesh makes it possible to work with high Reynolds numbers (turbulent field) and to reduce costs and time calculations .

In order to reach a better agreement with experimental results and to enable the treatment of diseases such as stenosis, regurgitation and prolapse, additional properties of valve tissues, are needed. Similarly, it is necessary to take into account the non-newtonian blood behaviour especially in the whirling area (coagulation phenomena). In this way, turbulence models from CFD modelling can be adapted to our system. Finally, certain geometries which function with 3 valves, aortic valves for example, will soon be envisaged by using simulations in 3 dimensions.

UNIVERSITY OF BIRMINGHAM

[1] Monaghan, J. J. (1992). "Smoothed Particle Hydrodynamics." Annual Review of Astronomy and Astrophysics 30: 543-574. [2] Monaghan, J. J. (2002). "SPH compressible turbulence." Monthly Notices of the Royal Astronomical Society 335(3): 843-852. [3] Liu, G. R. and M. B. Liu, Eds. (2003). Smoothed Particle Hydrodynamics: a meshfree method. [4] Morris, J. P., P. J. Fox and Y. Zhu (1997). "Modeling Low Reynolds Number Incompressible Flows Using SPH." Journal of Computational Physics 136(1): 214-226. [5] Monaghan, J. J. (1988). "Particle methods for hydrodynamics." Computer Physics Reports 3(1): 71-124. [6] Lucy, L. B. (1977). "A numerical approach to the testing of the fission hypothesis." Astronomical Journal 82(12): 1013-1024.

5th Annual BEAR PGR CONFERENCE 2014

Ab initio study of the effect of solute atoms on the vacancy diffusion in Ni-based superalloys

Kamal Nayan Goswami and Alessandro Mottura
School of Metallurgy and Materials, University of Birmingham, Edgbaston, Birmingham, B15 2TT, United Kingdom
Email: kng208@bham.ac.uk; a.mottura@bham.ac.uk

UNIVERSITY OF BIRMINGHAM

Ni-based superalloys

- High temperature components in jet turbine engines
- Two phase coherent γ/γ' structure
- Multicomponent systems - More than 10 alloying elements

- **Slow diffusing elements like Re improve the creep properties drastically at high temperatures**

The role of diffusion

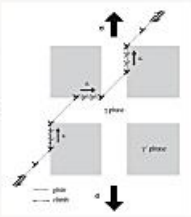

- Microstructure - High volume fraction of γ' precipitates surrounded by thin γ channels
- At high temperatures, dislocations don' t shear the hard γ' precipitates and deformation is restricted to softer γ channels
- Combined glide plus climb mechanism; rate-controlling step is the climb of dislocations at the γ/γ' interfaces
- Vacancy diffusion is essential for dislocation climb; its rate is dependent on the composition of the γ phase
- Most creep models show a direct dependence of the creep rate on an effective diffusion coefficient. However, different authors have used D_{eff} formulations which best fit their creep data.

$$\dot{\varepsilon}_{\langle 001 \rangle} \propto D_{eff} \quad ???$$

$$\frac{1}{D_{eff}} = \frac{x_1}{D_1} + \frac{x_2}{D_2} + \frac{x_3}{D_3} + \ldots\ldots + \frac{x_n}{D_n}$$

Inverse weighted average

$$D_{eff} = D_{0,eff} \exp\left[-\frac{Q_{eff}}{k_B T}\right] \qquad D_{0,eff} = \sum_i x_i D_{0,i} \qquad Q_{eff} = \sum_i x_i Q_i$$

Averaging the pre-factors and activation energies separately

- **Is vacancy diffusion coefficient an equivalent measure of the effective diffusion coefficient?**

Present Work

- Calculation of solute diffusion coefficients in Ni within dilute limits and estimation of D_{eff} from different models.
- Calculation of D_v from kinetic Monte Carlo simulations and verification of the D_{eff} models.
- Systems investigated: binary alloys of Re, W and Ta in Ni within dilute limits.

Calculating diffusion coefficients

- **The solute diffusion coefficients are given as,**

$$D_i = a^2 x_v f_i \Gamma_i$$

lattice parameter (3.52 Å); Atom – vacancy exchange frequency; Solute correlation factor; Equilibrium vacancy concentration

$$x_{v,i} = \exp\left(\frac{\Delta S_f}{k_B}\right)\exp\left(\frac{-\Delta H_{f,i}}{k_B T}\right) \qquad \Gamma_i = \nu^* \exp\left(\frac{-\Delta H_m}{k_B T}\right) \qquad f_i = \frac{2\Gamma_{ex} + 2\Gamma_{2ex}}{2\Gamma_{ex} + 2\Gamma_i + 7\Gamma_{2ex}}$$

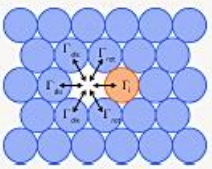

$$D_i = D_{0,i} \exp\left[-\frac{Q_i}{k_B T}\right]$$

- **Vacancy diffusion coefficients from Manning's random alloy model,**

$$D_v = a^2 \Gamma_v f_v$$

Average vacancy jump frequency; Vacancy correlation factor

$$\Gamma_v = x_i \Gamma_i + x_{Ni} \Gamma_{Ni} \qquad f_v = 1 - \frac{2}{7.15}\left\{\frac{9.15 x_{Ni} x_i (D_{Ni} - D_i)^2}{9.15(x_{Ni} D_{Ni} + x_i D_i)^2 - 2 D_{Ni} D_i}\right\}$$

- Assumption 1: The solvent, solute and vacancy distribution is random (i.e. no clustering or short-range ordering, no appreciable binding energy between solute and vacancy).
- Assumption 2: Jump frequency for an atom only depends on the atom and not the surrounding environment.

- **Kinetic Monte Carlo (kMC) simulations:**

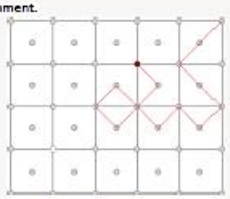

Diffusion coefficient by mean-square displacement

$$D = \frac{1}{6}\frac{\partial \langle R^2(t) \rangle}{\partial t}$$

- Simulates the most probable outcome of an event or a series of events through repeated random sampling.
- Under dilute approximation, 1 solute atom and 1 vacancy are present in a large system.
- The system size is varied from 15x15x15 unit cells to 3x3x3 unit cells to account for the solute composition variation from ~ 0 to 1 atom %.
- The different atom-vacancy jump rates are fed as inputs to the system and the system is allowed to evolve with time.

- **Computational Techniques used:**

- Ab-initio Density Functional Theory (VASP 5.3.2; GGA-PBE-PAW method). Convergence parameters: Energy cutoff = 400 eV, 5x5x5 k-mesh, Ionic forces < 10^{-2} eV/ Å.
- Nudged Elastic Band Method to calculate the enthalpies of migration (ΔH_m).

Results

Solute (i)	ΔS_f	$\Delta H_{f,i}$ (eV)	ν^* (10^{12} Hz)	ΔH_m (eV)
Ni	$1.4k_B$	1.44	2.57	1.08
Re	$1.4k_B$	1.48	1.67	1.48
W	$1.4k_B$	1.46	2.36	1.25
Ta	$1.4k_B$	1.36	2.56	0.755

Calculated terms for self diffusion and solute diffusion in Ni

		Re	W	Ta
Rotation	1 --> 1	1.13	1.20	1.37
	2 --> 3	1.12	1.11	1.10
	3 --> 2	1.04	1.08	1.12
	3 --> 3	1.07	1.06	1.05
	3 --> 4	1.07	1.07	1.08
	4 --> 3	1.15	1.16	1.18
Dissociation	1 --> 2	0.95	0.97	1.01
	1 --> 3	1.07	1.04	1.00
	1 --> 4	1.06	1.05	1.02
Association	2 --> 1	1.05	1.00	0.89
	3 --> 1	1.08	1.04	0.91
	4 --> 1	1.14	1.13	1.02

ΔHm for different Ni jumps in the vicinity of solute atoms used in the kMC simulations. Numbers indicate the nearest neighbour position of the vacancy with respect to the solute atom

Solute diffusion coefficients and Effective diffusion coefficients

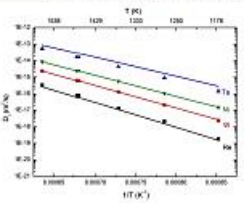

Solute diffusion coefficients in Ni as a function of Temperature from analytical formulations (lines) and kMC simulations (symbols)

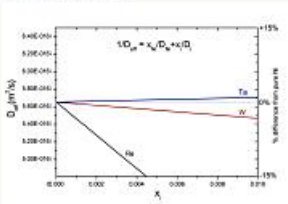

Effective diffusion coefficient in Ni at 1373 K using inverse weighted average method

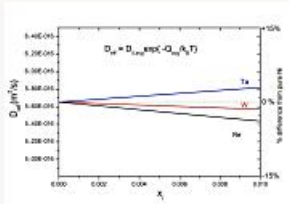

Effective diffusion coefficient in Ni at 1373 K by averaging the diffusion pre-factor and activation energies separately

Vacancy diffusion coefficients from Manning's model and kMC simulations

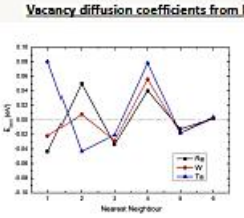

Low magnitudes of solute-vacancy binding energies indicating random distribution in dilute alloys

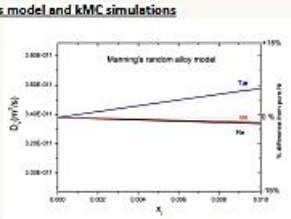

Vacancy diffusion coefficient at 1373 K using the Manning's random alloy model

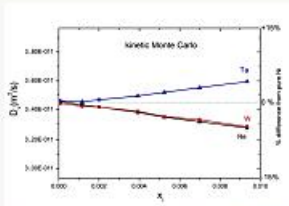

Vacancy diffusion coefficient at 1373 K from kMC simulations

Discussion

- Solute diffusion coefficients calculated from analytical formulations overlapped those calculated from kMC simulations. Re, as expected, was found to be the slowest diffusing solute amongst the three. Ta was the fastest.
- The different models for D_{eff} don't agree to each other. The inverse weighted average model predicts that the slower diffusing atom is rate controlling, while the other model shows a much smaller effect.
- The Manning's random alloy model predicts almost negligible effect for both Re and W in terms of reducing the D_v as compared to pure Ni. However, the validity of this model is undermined by its various simplifying assumptions.
- kMC simulations show that an addition of 1 at. % of both Re and W decrease the D_v by ~ 5 %. This effect is minimal, and may not be enough to explain the creep strengthening attributed to these elements.
- Calculation of diffusion coefficients in non-dilute systems, accounting for solute-solute interactions, is required to get a complete picture.
- Vacancy absorption / emission at the dislocation cores could be the rate controlling step in dislocation creep in Ni-based superalloys.

Future Work

Work is underway to extend the present investigation to non-dilute systems using a combination of cluster expansion methods and kinetic Monte Carlo simulations. The results from the non-dilute regime should conclusively determine the role solute elements play in the vacancy diffusion in Ni-based superalloys.

References

[1] R. Reed, The Superalloys: Fundamentals and Applications, Cambridge University Press, UK (2006).
[2] Z. Zhu, H. Basoalto, N. Warnken and R. Reed, Acta Materialia, 60 (12) (2012), pp. 4888–4900.
[3] A. Heckl, S. Neumeier, M. Göken and R. Singer, Materials Sciencs and Engineering A, 528 (9) (2011), pp. 3435–3444.
[4] A. Lidiard, CXXXIII., Philos. Mag. Ser. 746 (382) (1955) 1218–1237.
[5] J.R. Manning, Phys. Rev. B, 4 (1971), pp. 1111–1121.
[6] K. N. Goswami and A. Mottura, Materials Science and Engineering A, 617 (2014), pp. 194-199.

Acknowledgements

The authors would like to acknowledge the use of the BlueBEAR High Performance Computing facility at the University of Birmingham for the calculations presented above. The authors would also like to thank Prof. Ralf Drautz, Dr. Jutta Rogal and Dr. Sergej Schuwalow of the Interdisciplinary Centre for Advanced Materials Simulation at the Ruhr-Universität, Bochum in Germany for the valuable discussions.

Geometry and Conferred Ordering Within Hydrated Perchlorate Clusters

John C. Hey, Lewis C. Smeeton and Roy L. Johnston
JCH936@bham.ac.uk

UNIVERSITY OF BIRMINGHAM

Introduction

Perchlorate is a chaotropic Hofmeister ion, it disrupts the stability and solubility of proteins in water.
It has been shown that sulfate ions, (kosmotropes), impart long range order to water clusters,[1] and somewhat simplify their energy landscapes.[2]
In this work we present putative global minima for the $(ClO_4^-)(H_2O)_N$ system ($N \leq 16$), as well as a study into the ordering conferred to water by the presence of a perchlorate ion, and a comparison of this effect with that of the equivalent sulfate systems, as evidenced by the suppression of hydroxyl groups normal to the surface of the cluster.

Geometry Optimisation

Basin hopping geometry optimisation using an empirical potential (**1**) which includes a Lennard-Jones and a coulombic component, through the pele[3] software package.

$$U = \sum_{i=1}^{N} \sum_{j=i+1}^{N} \left\{ \frac{q_i q_j}{r_{ij}} + 4\epsilon_{ij} \left[\left(\frac{\sigma_{ij}}{r_{ij}} \right)^{12} - \left(\frac{\sigma_{ij}}{r_{ij}} \right)^{6} \right] \right\} \quad (1)$$

Where U is interaction energy, q_i and q_j are the charges on sites i and j, r_{ij} is the distance between i and j, and ϵ_{ij} and σ_{ij} are the pairwise Lennard-Jones terms for sites i and j.
TIP4P four body water model used with perchlorate potential derived from LCAO MO SCF from the literature.[4] All molecules modelled as rigid bodies to make moves and minimisations inexpensive.
Three move-classes in 100 move blocks. Rotations, Translations and Cycle-Inversions.

Putative Global Minima

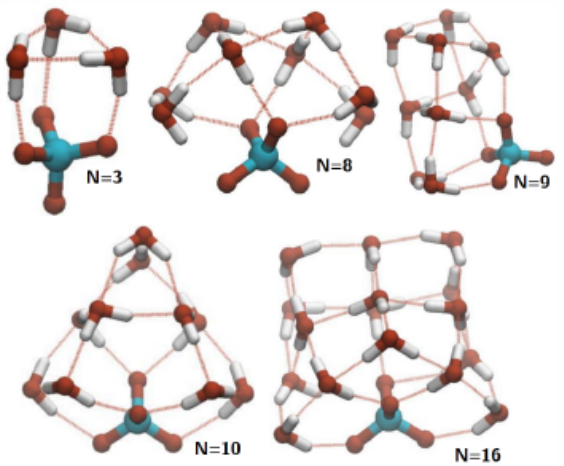

Figure 1: Selected putative global minima for the $(ClO_4^-)(H_2O)_N$ System

Conferred Order

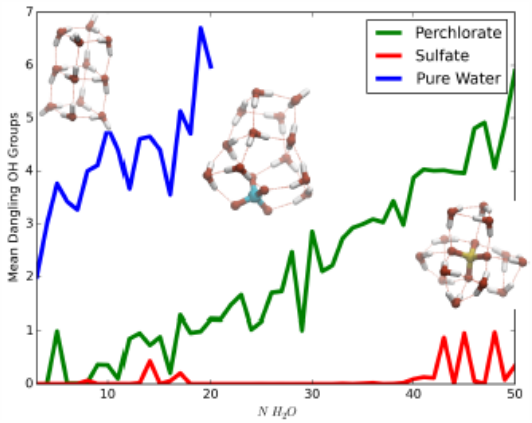

Figure 2: Boltzman weighted mean number of hydrogen bonds normal to the surface and putative global minima for $(H_2O)_{12}$ for the Pure Water, Hydrated Perchlorate and Hydrated Sulfate systems highlighting the morphological differences between the three systems.

Conclusions

- Good candidate global minima have been presented for $(ClO_4^-)(H_2O)_N$ with $N \leq 16$.
- Unlike sulfate, perchlorate favours interfacial sites. Perchlorate displays structural motifs seen in pure water clusters.
- Perchlorate confers some patterning to water clusters, this is supported by the suppression of dangling hydrogen bonds.

References

[1] J. T. O'Brien, J. S. Prell, M. F. Bush and E. R. Williams, *JOURNAL OF THE AMERICAN CHEMICAL SOCIETY*, 2010, **132**, 8248–8249.

[2] L. C. Smeeton, J. D. Farrell, M. T. Oakley, D. J. Wales and R. L. Johnston, *JOURNAL OF CHEMICAL THEORY AND COMPUTATION*, 2015, **11**, 2377–2384.

[3] J. Stevenson and V. Ruehle, *PELE, the Python Energy Landscape Explorer*, https://github.com/pele-python/pele.

[4] G. HEINJE, W. LUCK and K. HEINZINGER, *JOURNAL OF PHYSICAL CHEMISTRY*, 1987, **91**, 331–338.

UNIVERSITY OF BIRMINGHAM EPSRC

Acknowledgements

We would like to thank the EPSRC for funding under program grant EP/I001352/1. Computational facilities were provided by MidPlus and the University of Birmingham's BlueBear HPC service.

Parametric Finite Element Model of The Human Lumbar Spine.

C. E. Lavecchia, DM. Espino, D. ET Shepherd

School of Mechanical Engineering, University of Birmingham

Introduction

The World Health Organisation and the Global Burden of Disease recognises low back pain as one of the major cause of disability worldwide. Much focus is on the development of new devices to preserve the range of motion of the spine and to restore quality of life. However, evaluating the performance of these devices, once implanted in the human body, is still challenging. A method largely used in biomechanics fields is to evaluate the biomechanical behaviour of the spine using Finite Element Models.

The aim of this study was to develop a parametric model of the lumbar spine, enabling evaluation of spinal implants and their effect on the biomechanics of the spine. The parametric model was based on a model supplied by an industrial collaborator (S14 Implants, Pessac, France), and it allows models to be reconstructed for patients with different heights and ages .

Model development

The parametric model was developed using Matlab, sampling data from the original model and fitting the external surfaces using polynomial fitting (Fig.1).

Geometrical parameters, to describe the vertebrae shape, were defined and functions found in literature have been used to correlate those parameters (Fig.2). For example, it is possible to correlate the posterior vertebral height to the height of a patient (Fig.3) . Following correlation analyses, a Matlab script has been written in order to automatically obtain the complete lumbar model (L1-L5 vertebrae).

Finally, the vertebrae has been organised in 3D space considering the gaps for the intervertebral discs, which can vary with the subject's age, and their orientation following the Cobb's angle (Fig.4).

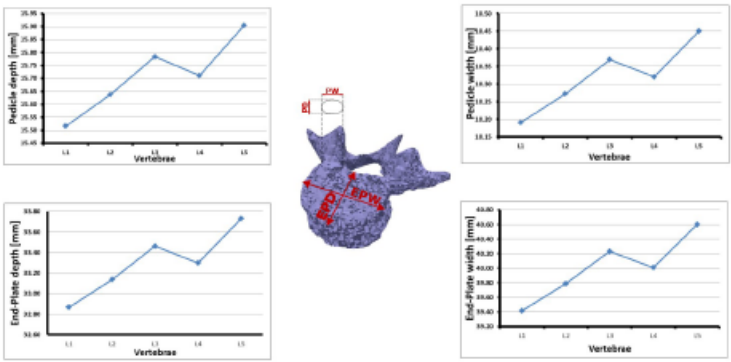

Figure 2. Dimensions of each vertebrae for a 30 year old subject, 177cm in height.

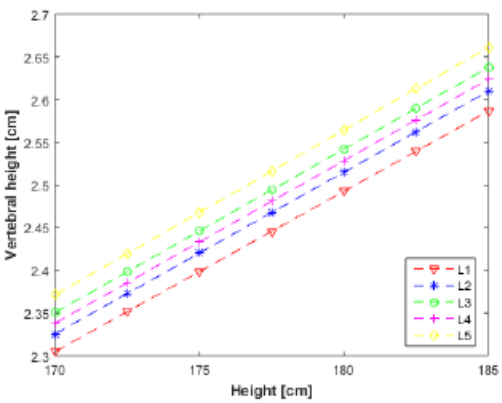

Figure 3. Variation of the posterior vertebral height (L1 to L5) with the height of a person.

Achievements

The parametric model allows reconstructing a model for subjects with different heights and ages. As first approximation, only certain geometrical parameters were taken in account. Nevertheless, it allows five parameters to be modified for each vertebrae and one parameter for the intervertebral disc (correlated to the patient's age) in the lumbar region, making a total of thirty parameters for each subject. Moreover, as the model's dimensions are user controlled, it is possible to define different regions of vertebrae in order to apply the correct regional material properties to the Finite Element Models (e.g.: trabecular or cortical bone).

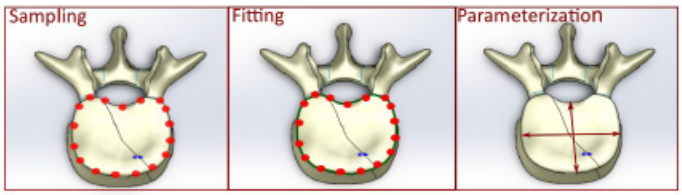

Figure 1. Model development workflow.

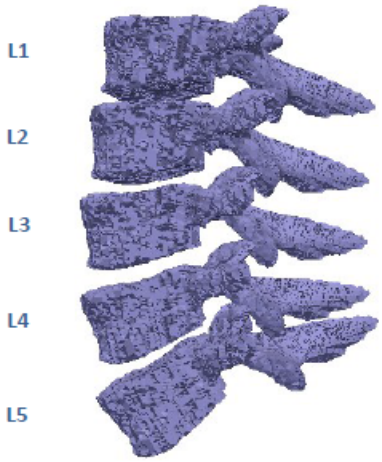

Figure 4. Lumbar vertebrae for a 30 year old subject (height: 177cm). The intervertebral discs' heights, and consequently the gaps between each vertebrae, are influenced by the age of a subject, while the inclination of each vertebra is related to the Cobb's angle.

Figure 5. Finite Element Model of a functional unit (L4-L5 and intervertebral disk) extracted from the original model. On the left the functional unit without device and on the right the L4-L5 with BDyn, device produced by the S14 Implants.

Conclusion & future work

This parametric model developed enables sensitivity analysis on geometric parameters, so ad to understand the influences of morphological parameters on the biomechanics of the spine. Furthermore, this model will be used to evaluate the influence of spinal implants on the biomechanics of the lumbar spine (Fig.5) .

Acknowledgments

The authors would like to thank the S14 Implants and Bernard Lawless for his advices. This study was supported by the European Commission under the 7th Framework Programme (Grant agreement no.: 604935).

UNIVERSITY OF BIRMINGHAM

Polymer Technology Group

The friction coefficient and wears mechanisms of PEEK and PEEK composite in water lubricated sliding contacts

Zainab shukur and Karl Dearn
School of Mechanical Engineering University of Birmingham

Abstract

The friction coefficient and wears mechanisms of PEEK and PEEK composite running against bearing steel in reciprocating sliding contacts has been investigated in dry lubricated and water lubricated conditions. Experiments explored how the lubrication state, load and rotational speed influenced the tribological performance of the polymers. Tribological tests were conducted on a TE77 high frequency tribometer, running in a ball-on-plate configuration and cylinder-on- plate configuration, scanning microscopy was used to investigate the wear mechanisms.

Highlights

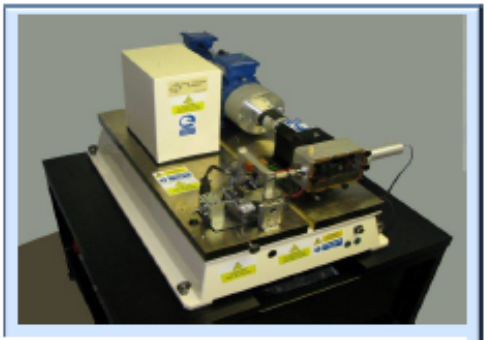

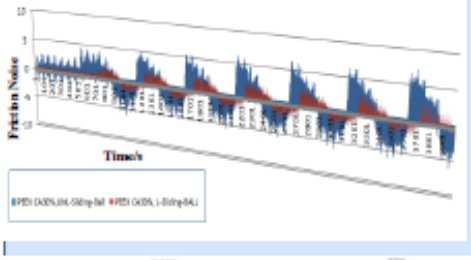

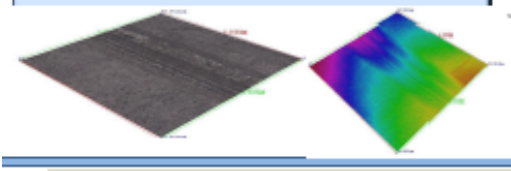

Results

Standerd9s0: ISO 4287; ISO 11562; ASME B46. 1-2002 (Refer to the help for information)

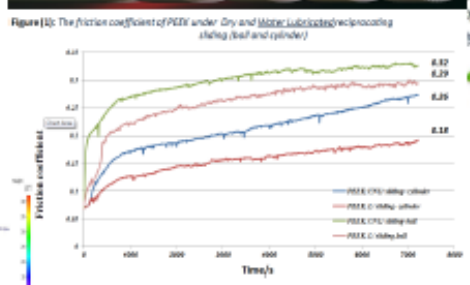

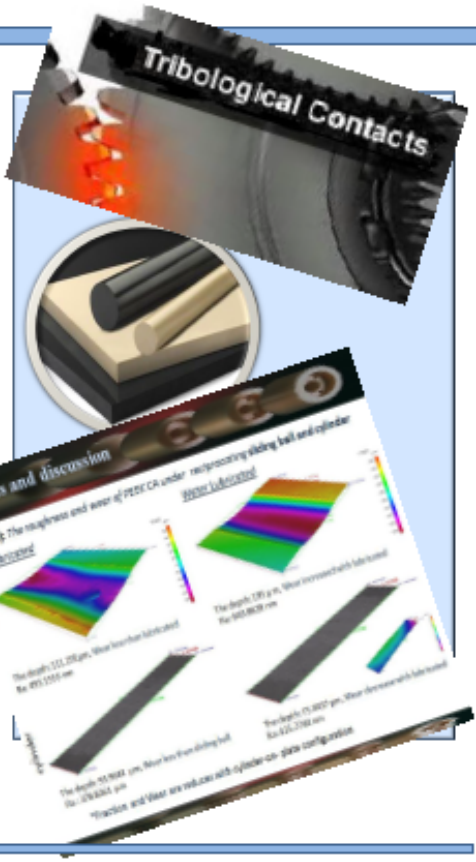

Discussion and Conclusions

The friction coefficient and wears mechanisms of PEEK and PEEK composite running against bearing steel in sliding. contacts has been investigated in dry lubricated and water lubricated conditions It was observed that the wear for the composite PEEK was reduced when compared against unreinforced PEEK, under both lubricated and dry conditions. When water lubricated, although the composite showed the lowest wear and friction, tribological performance was improved for both materials. The tribological properties of the friction coefficient of composite were less sensitive to operating parameters under water lubricated condition, compared to the unreinforced polymer.

- Tribological properties of PEEK composites are best suited to lubricated application.
- Higher contact pressures reduce coefficient of friction but increase wear.
- Friction coefficient is reduced in (cylinder-on-plate configuration) fretting at the same properties with ball plate configuration.
- The friction nosie contact reduce with lubricated.
- Material has been spread across surface at dry lubricated.
- Friction reduced with higher load

Finite Element Modelling of CRUD Deposition in Nuclear Plant utilising COMSOL Multiphysics

Jiejie Wu[a], Nathan Johnson[a], Jonathan Morrison[a], Brian Connolly[a]

a. Department of Metallurgy and Materials, University of Birmingham, Edgbaston, Birmingham, B15 2TT

Introduction

The elimination of CRUD deposition in PWR power plants is an area that is of great interest to the nuclear industry, due to its ability to cause: TSP blockage, tube failure, radioactive species incorporation, fuel leakage...

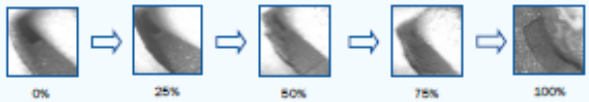

TSP Blockage in Cruas Nuclear Plant, France, 2004 - 2006

Theory (Fluid dynamics + Electrochemistry + ...)

Deposition at flow restrictions is believed to be caused by electrokinetic wall currents driving the electrochemical reactions forming magnetite deposits at the restrictions. The two half equations are:

$3Fe^{2+} + 4H_2O \rightarrow Fe_3O_4 + 8H^+ + 2e^-$

$H_2 \rightarrow 2H^+ + 2e^-$

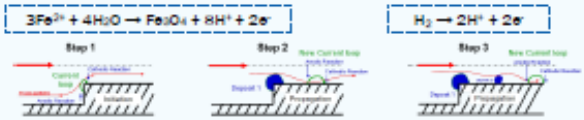

Initial deposit followed by discrete annuli

Methodology

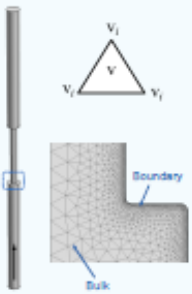

- Finite Element Method (FEM)
  - Split the domain into a finite number of *vertices* (x_i, y_i)
  - Only solve for a finite number of unknowns $v_i = v(x_i, y_i)$
  - Approximation: $v_i \rightarrow v$
- Mesh
  - Boundary: quadrilateral mesh
  - Bulk: triangular mesh

Mesh Sweep

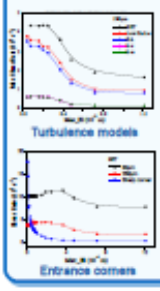

Turbulence models

Entrance corners

- Mesh sweep, *3.68E-5m* to *0.00121m*, has been studied for five turbulence models
- Shear rate decreases with increasing mesh size
- The k-ε and k-ω models gave lower shear rate due to wall function in boundary layer
- A sharp corner is not an ideal geometry for the flow passing through vena contracta

Deposition Built-Up Rate

- Parameters: *12 m/s, 290°C, 3 days*
- Turbulence model: *Shear-Stress Transport (SST)*
- Deposition location: *inlet, 23mm, 38mm, outlet*
- $Height_{max}$ = *46.3 μm*; $Height_{ave}$ = *19.3 μm*
- Ripple distance: *~100 - 200 μm*
- BUR = *4.20E-4 g m^{-2} s^{-1}* (*4.93E-4 g m^{-2} s^{-1}*, J. McGurk, 2012)

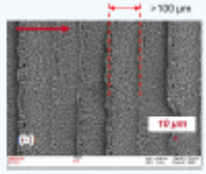

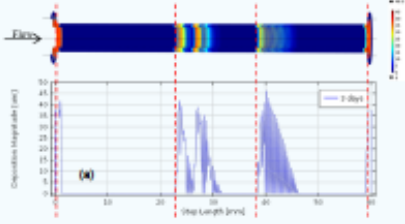

(a) Deposition magnitude along restriction step, 3 days; (b) Guillodo, 2009

Velocity and Shear Rate

- Recirculation zone: adjacent to the entrance
- Velocity direction changes in boundary layer

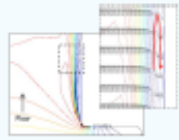

Recirculation zone

- Shear rate dominates the streaming current which drives the deposition process

$$I_s = -2\pi a \varepsilon \varepsilon_0 \zeta (du/dy)_0$$

- Fluctuations of shear rate are located where the deposition happens
- Maximum (*7.24E5/s*) - restriction entrance

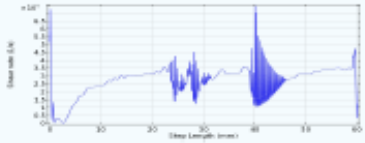

Shear rate along restriction step, 3 days

Pressure Drop

- Pressure drop in restriction is believed to be caused by the deposit ripples
- Head loss variations have been observed in nuclear plants and lab tests

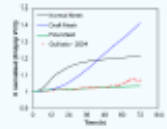

Pressure drop, 3 days

Experimental

- A bespoke rig of plant scale with the same restriction size
- Experimental work will be used to do data comparison
- Deposits found are rich in antimony from EDX analysis
- T influences morphology
  - High T - crystalline structure
  - Low T - hard wall-like deposits

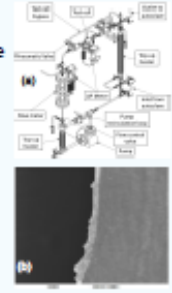

(a) Rig - Hot loop;
(b) Deposits observed

Conclusions

- Mesh size is an important factor influencing deposition magnitude;
- Most of the deposits are located at the entrance of restriction;
- A recirculation zone is found adjacent to the entrance;
- Shear rate fluctuations are located where the deposition happens;
- Build-Up Rate is comparable to J. McGurk's test

References

[1] N. Lostec, Y. Kernin, C. Ferre, J. Martens and D. Dumay. "Tube Support Plate Clogging and Secondary Side Deposit: Performance Evaluation Using Simulation and Site Results."

[2] C. Brun, N. Engler, G. Berthollon, T. Muller and B. Sala, "Investigation on the Relation Between Pressure Drops and Fluid Chemical Treatment," in *Water Chemistry of Nuclear Reactor Systems 5*, 1989.

[3] M. Guillodo, T. Muller, and M. Barale, "Singular Deposit Formation in PWR due to Electrokinetic Phenomena – Application to SG Clogging," in *6th CNS International Steam Generator Conference Proceedings*, 2009.

Acknowledgement

I would like to thank to CSC and University of Birmingham for the funding of the project. Also, I would like to thank to my supervisor, Dr Brian Connolly, for his guidance and support.

Additional Information

Jiejie Wu, PhD student

Metallurgy and Materials, UoB

jxw465@bham.ac.uk

Application of a ghost fluid approach for a multiphase lattice Boltzmann method

Wenxin Zuo[1], Andrew Chan[2] and John Bridgeman[1]
1 School of Civil Engineering, University of Birmingham, UK
2 School of Engineering, University of Tasmania, Australia

Research Objectives

Two-phase fluid flow at large density ratio (~1000:1) in porous media occurs in many environmental and industrial processes. The Lattice Boltzmann (LB) Method, unlike the traditional numerical approaches, provides a convenient means to simulate multiphase fluid flow on curved solid particles with true geometry. But the widely used boundary condition in multiphase LB model requires large grid resolution to capture meniscus movement on it, while others are unable to ensure mass conservation in the computation. Therefore, the objectives of my project are to:

- Develop a modified boundary approach incorporated with Lee's LB model
- Validate the new boundary model with smaller grid resolution
- Analyse the mass conservation in the computation

Numerical Method

Governing equations for LB model

The Discrete Boltzmann Equations (DBE):

$$\partial_t f_i + \boldsymbol{e}_i \cdot \nabla f_i = -\frac{f_i(\boldsymbol{x},t) - f_i^{eq}(\boldsymbol{x},t)}{\lambda} + \frac{(\boldsymbol{e}_i - \boldsymbol{u}) \cdot (\boldsymbol{F} + \boldsymbol{G})}{\rho c_s^2} f_i^{eq}(\boldsymbol{x},t)$$

$$f_i^{eq} = \omega_i \rho \left[1 + 3(\boldsymbol{e}_i \cdot \boldsymbol{u}) + \frac{9}{2}(\boldsymbol{e}_i \cdot \boldsymbol{u})^2 - \frac{3}{2}\boldsymbol{u} \cdot \boldsymbol{u}\right]$$

The modified distribution equations in Lee's LB model:

$$g_i = f_i c_s^2 + (p - \rho c_s^2)\Gamma_i(\mathbf{0})$$

$$h_i = (C/\rho) f_i$$

The new collision equations are:

$$\bar{g}_i = g_i + \frac{1}{2\tau}(g_i - g_i^{eq}) - \frac{\delta t}{2}(\boldsymbol{e}_i - \boldsymbol{u}) \cdot \left[\nabla \rho c_s^2 \cdot (\Gamma_i(\boldsymbol{u}) - \Gamma_i(\mathbf{0})) + (-\rho g \nabla h + \mu \nabla C) \cdot \Gamma_i(\boldsymbol{u})\right]$$

$$\bar{h}_i = h_i + \frac{1}{2\tau}(h_i - h_i^{eq}) - \frac{\delta t}{2}(\boldsymbol{e}_i - \boldsymbol{u}) \cdot \left[\nabla C - \frac{C}{\rho c_s^2} \cdot (\nabla p_b - \mu \nabla C + \rho g \nabla h)\right]\Gamma_i(\boldsymbol{u})$$

Ghost Fluid approach

The value of the Ghost Points (GP) is extrapolated from the value of Image Points (IP).

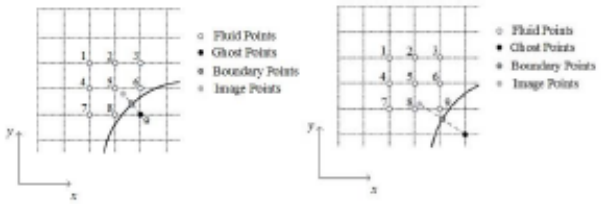

The bi-quadric interpolation scheme used in the model to calculate the value of Image Points (IP)

$$\varphi = ax^2y^2 + bxy^2 + cx^2y + dx^2 + ey^2 + fxy + gx + hy + k$$

Numerical Results

1. Capillary Rise

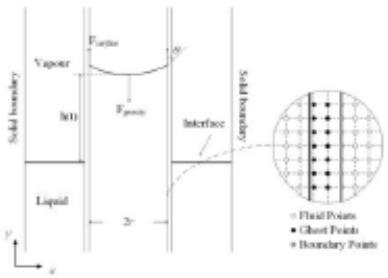

The theoretical capillary rise is $h = \frac{\sigma \cos\theta}{\rho r g}$

The parameters in the capillary rise test

Parameter	Physical units	Lattice units
Lattice unit length	5.0×10^{-5} m	1.0
Time step	1.0×10^{-6} s	1.0
Liquid density	997.1 Kg/m^3	1.0
Gas density	1.177 Kg/m^3	1.18×10^{-3}
Liquid kinematic viscosity	8.926×10^{-7} m^2/s	3.570×10^{-4}
Gas kinematic viscosity	1.568×10^{-5} m^2/s	6.272×10^{-3}
Surface tension	0.072 N/m	5.777×10^{-4}
Contact angle	60°	60°
Gravity	9.8 m/s^2	1.960×10^{-7}

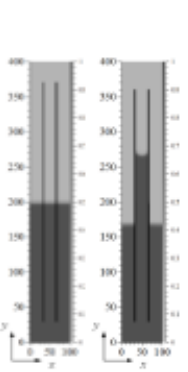

Component contours of capillary rise at initialization and steady state

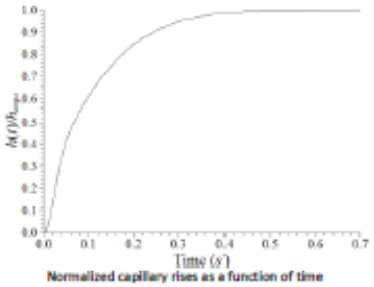

Normalized capillary rises as a function of time

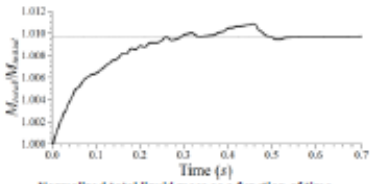

Normalized total liquid mass as a function of time

2. Capillary Bridge

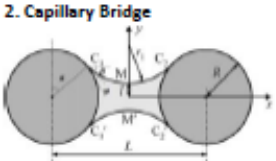

Sketch of capillary bridge between the two circular bodies

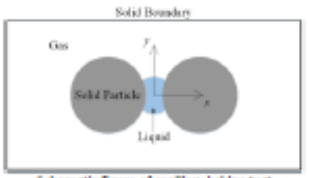

Schematic figure of capillary bridge test

The parameters in the capillary bridge test

Parameter	Physical units	Lattice units
Lattice unit length	1.0×10^{-4} m	1.0
Time step	1.0×10^{-6} s	1.0
Liquid density	997.1 Kg/m^3	1.0
Gas density	1.177 Kg/m^3	1.18×10^{-3}
Liquid kinematic viscosity	8.926×10^{-7} m^2/s	8.926×10^{-5}
Gas kinematic viscosity	1.568×10^{-5} m^2/s	1.568×10^{-3}
Surface tension	0.072 N/m	7.222×10^{-5}
Contact angle	30°	30°
Particle radius	3.079mm	30.79

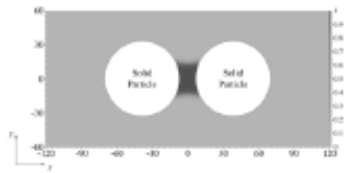

Component contour at 0.3s

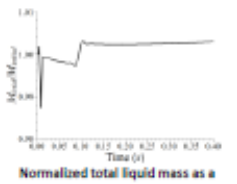

Normalized total liquid mass as a function of time

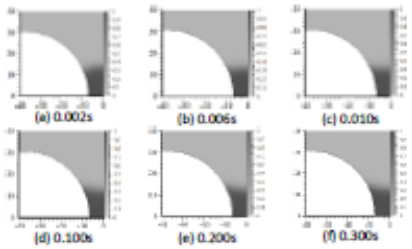

The evolution of component contour at first 300,000 time steps (0.3s)

Conclusion

The new algorithm was validated with two theoretical tests: the capillary rise test and the capillary bridge test. The numerical results were shown to be consistent with analytical solutions in both tests. Mass conservation was observed to within 1%. In the future, it is anticipated that the new approach will provide a novel way to incorporate LB models with other numerical methods, such as the discrete element method, in realistic problem analysis.

Notes

Notes

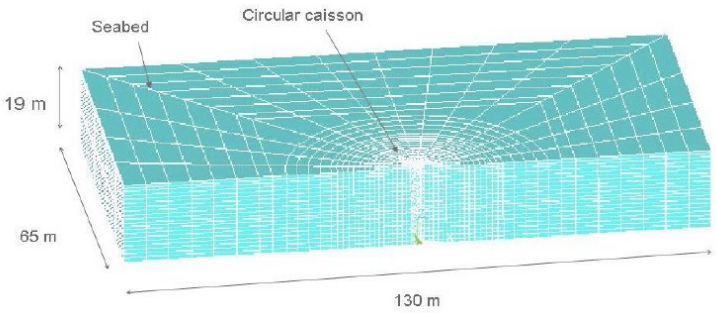

Three-dimensional Numerical Modelling of Dynamic Saturated Soil and Pore Fluid Interaction – Jianhua Ou, Department of Civil Engineering

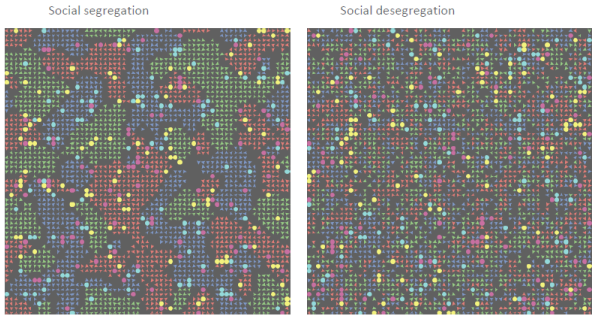

Agent-based modelling of social phenomena - Gregory Carslaw, School of Psychology

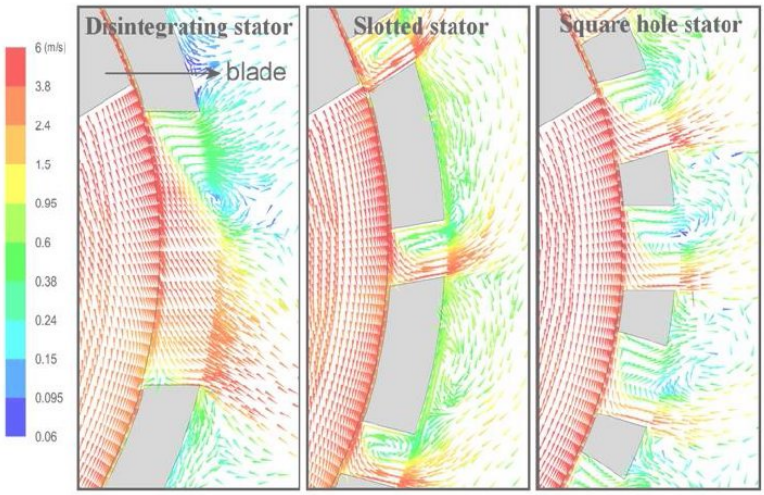

High shear rotor-stator mixers - Dr Adi Utomo, Department of Chemical Engineering

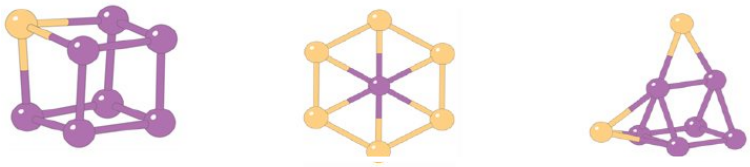

Parallel Genetic Algorithms for Structural Characterisations of Nanoalloys - Jack Davis, School of Chemistry

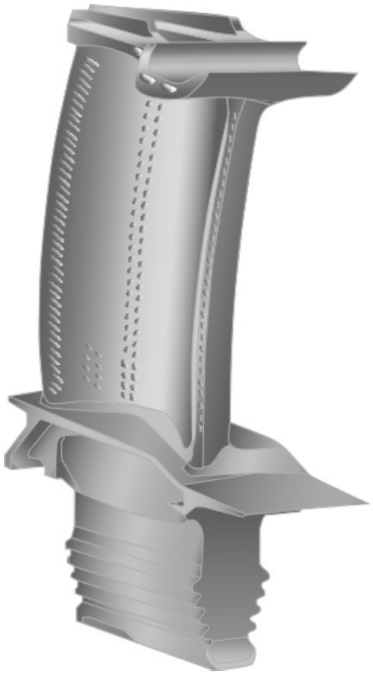

Modelling the heat treatment of single crystal nickel based superalloys – Francesco Cosentino, School of Metallurgy and Materials

BEAR PGR Conference Organising Committee 2015

Shaun Evans (Chair)

Fiona Schulz (Secretary)

Fadhil Alfarag

Zainab Alsharify

Saif Alzabeebee

Dominic Flynn

Earl Jones

Ika Ikrom